

## 1 Risk Model

Risk is modelled as a function,  $\mathbb{R}^3 \rightarrow [0, 1]$  which is used to determine the risk at every  $(x, y, z)$  location within the search space. In order to determine risk in 3-space, we obtain a 2-D risk model which models the risk at the minimum altitude. This function  $R_0 : \mathbb{R}^2 \rightarrow [0, 1]$  determines what the risk would be at the minimum altitude. This is assumed to be given to the algorithm *a priori* or can be determined at any time during the iteration of the algorithm. This ground risk,  $R_0$ , is modelled as a lookup table rather than a combination of basis functions in order to give a more generic model for risk that can be used in any use case of the algorithm. To determine the 3-D risk,  $R(x, y, z)$ , we perform an exponential decay on the given ground risk value,  $R_0(x, y)$ . 3D risk is defined as follows:

$$R(x, y, z) = R_0(x, y) \cdot \exp\left(-\frac{z^2}{K \cdot R_0(x, y)^2}\right)$$

Even though risk in 3D is evaluated and is not simply a lookup table, one can be used instead. This representation for 3D risk is ideal for modelling fires, detection by hostile agents, or any stimuli that would decrease monotonically as the altitude increases.

For the experiments, we have used nine different scenes for the representation of the ground risk,  $R_0$ . To generate these scenes, we used the diamond-square algorithm [1] to generate random terrain maps that have values from zero to one. The diamond-square algorithm generates realistic random risk scenes that represent the 2D ground level risk as anticipated. Random terrain maps have also been used in [2] to represent random risk for path planning problems. A heat-map showing a random terrain map generated with the diamond square algorithm is shown in Fig 1.

## 2 2D Planning

Quadruped robots use a very simple, reactive rule to determine where to move that has extremely emergent properties. Given a map,  $M$ , quadruped robots move to areas with a combination of the largest uncertainty,  $\Upsilon$ , and the lowest risk,  $R$ . Our implementation uses a cost surface that is shared between members of the swarm. Since the quadruped robots update this cost surface as they move around it, the cost surface is used as the mode of communication between the quadruped robots. This cost surface removes the need for the agents to have any peer to peer communication and also removes the need for any agent to have perfect information about the swarm.

For a quadruped robot to determine a new heading, the agent samples costs from the surface around the edge of its sensor footprint. It then moves in the direction of the smallest cost. Once it has moved, the agent updates the measurements for the uncertainty grid,  $\Upsilon$  for the area that was just covered in by the sensor footprint. This uncertainty update happens iteratively in the swarm, so the

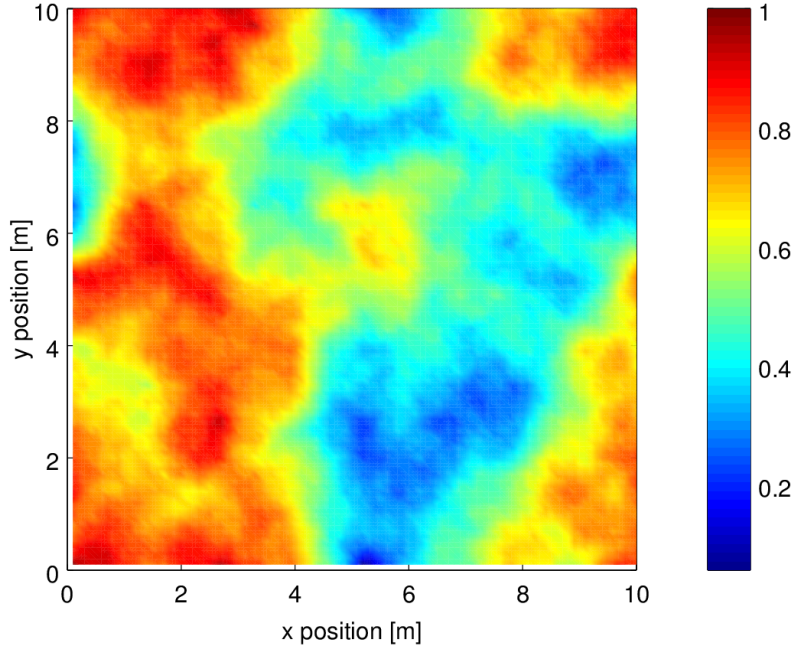


Figure 1: A visualization of the ground risk,  $R_0$

quadrotors left the plan their movements have an updated grid before they determine a new heading.

The cost surface,  $\Gamma$ , is made up of a combination of the uncertainty grid,  $\Upsilon$  and the risk surface of the region. More formally, assume that there is a function  $\delta : \mathbb{R}^2 \rightarrow \mathbb{R}$  which is used to combine the uncertainty and risk into one metric. This is assumed to be a user defined function which may change from application to application. The cost surface is then defined as,

$$\Gamma(x, y) = \delta(\Upsilon(x, y), R(x, y))$$

For our implementation we defined  $\delta$  as,

$$\delta(v, r) = \max \Upsilon - v + 100 \cdot r$$

An instance of the uncertainty surface,  $\Upsilon$ , is shown in Fig 2 where the  $x, y$  coordinate represents the 2D position within the workspace and the color represents the level of uncertainty. Notice the two dark blue ellipses with low uncertainty. That is the current sensor footprint of the quadrotors at the time at which the snapshot was taken. Fig. 2 shows a snapshot of the cost surface which is created by combining the risk surface shown in Fig. 1 and the uncertainty surface shown in Fig. 2 using the  $\delta$  combination function used in our implementation.

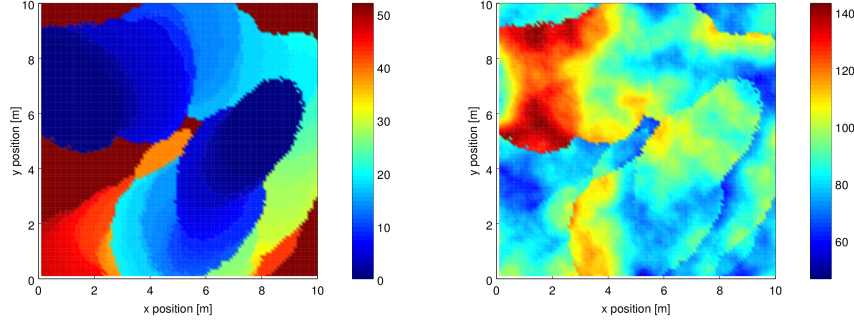


Figure 2: The two images show the uncertainty surface and the cost surface respectively. The cost surface is a combination of the risk shown in Fig. 1 and the uncertainty surface.

Fig. 3 shows snapshots of the algorithm in sequence. The figures show iteration 1, 25, 50, and 100. These figures show the representation of the uncertainty surface and the cost surface. As the algorithm progresses the uncertainty of the area changes and so does the associated cost. These surfaces are vital for the planning of the quadrotors.

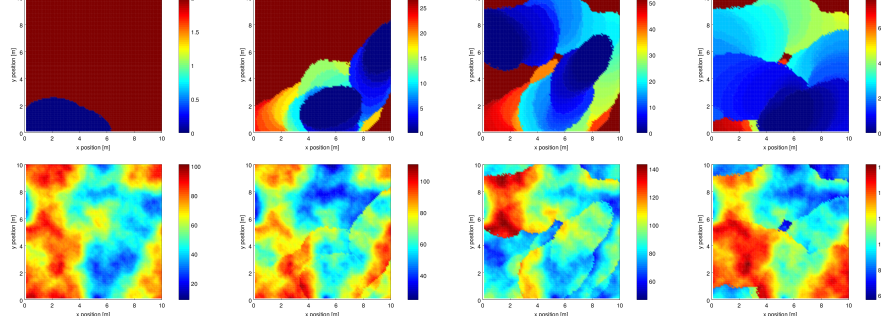


Figure 3: Shows how the uncertainty surface and the cost surface change as the algorithm progresses. These surfaces are used to determine the new position of the quadrotors

Fig. 4 shows how the quadrotors fill the space whilst reducing the frequency of visit to high risk areas whilst maintaining persistent coverage over low risk areas. This figure is a sequence of images that shows how the algorithm progresses.

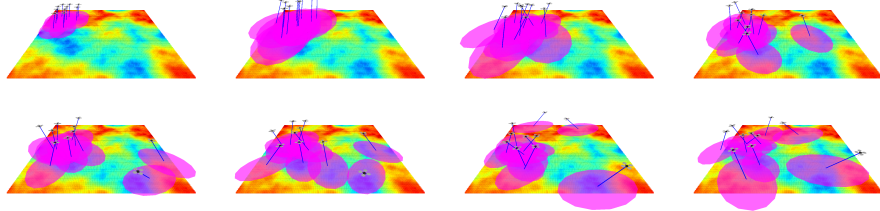


Figure 4: Shows how the quadrotors move to fill the search space whilst trying to avoid the frequency of visit to areas of high risk using 10 agents

### 3 Results & Discussion

To determine how well Rover performed, we constructed three different experiments that tested various attributes about the implementation. We have also gathered four different metrics to show the performance of the implementation. To gather the experimental data, we decided to use three different scene sizes. For each of the scene sizes, we used 3 different ground risk surfaces created using the diamond square algorithm. The experiments developed are described below and after each description is the associated data and discussion.

#### 3.1 Metrics

The metrics that we are gathering in the experiments are used to show that the algorithm minimizes risk, maximizes the sensor quality, fills the search space quickly and persistently, and that the algorithm can be used in a real time setting. The metrics that are being collected are the average associated risk, the average associated sensor quality, the average amount of iterations it takes to reach 90% cumulative coverage, and the amount of time per iteration.

##### 3.1.1 Average Associated Risk

This metric describes the average risk incurred by the quadrotors. Each of quadrotors is experiencing some sort of risk. By averaging the risk associated with each of the quadrotors, we are able to quantify how much risk is being incurred by the swarm. By showing that this metric remains low, indicates that the algorithm is completing its proposed task.

##### 3.1.2 Average Associated Sensor Quality

The average associated sensor quality was acquired by breaking the workspace into a grid. For each cell in the grid, we record the maximum sensor quality out of all the quadrotors that are currently viewing that cell. For a unified metric, we then average all the sensor quality values for all the grid cells that are currently being covered. This gives an accurate representation of the average sensor quality for the swarm.

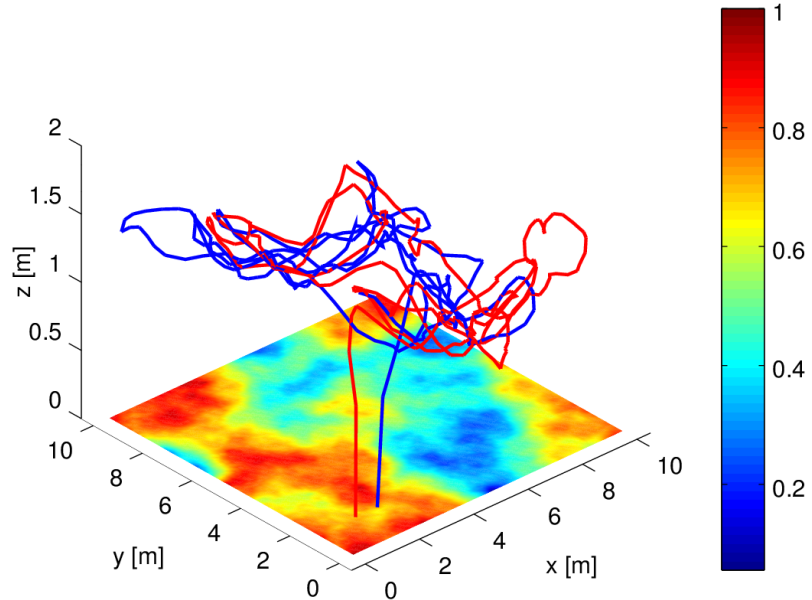


Figure 5: Shows the trajectories of two quadrotors (the red and blue lines) performing the algorithm through the search space. Notice that the quadrotors stay in low risk areas and increase their height above the high risk regions.

### 3.1.3 Persistent Cumulative Coverage

To show that the proposed approach persistently covers the search area, we gathered the number of iterations for the algorithm to reach 90% cumulative coverage throughout progression of each run. This means that once the algorithm reached 90% cumulative coverage, we recorded the number of iterations it took, and reset the cumulative coverage back to zero. We then averaged the number of iterations it took. This is a good metric for showing persistent coverage because it captures how long it takes for the agents to fill the space from many different initial configurations. If there is a low deviation between the values, then we know that the initial configurations of the quadrotors had little to no effect on the persistence of coverage. Also, this metric can be used to determine how quickly the quadrotors filled the area on average. This becomes the standard performance metric used for the algorithm.

### 3.1.4 Time per Iteration

Since this algorithm is to be used in a real-time setting, we need to show that each iteration (or each update of the quadrotors' positions) shouldn't take too

long. This metric shows the feasibility of the approach in a real-time scenario.

### 3.2 Performance as function of the number of quadrotors

To determine the performance as a function of the number of quadrotors in the swarm, we ran the algorithm for 1000 iterations on each of the nine scenes using a swarm size of  $1, 5, 10, \dots, 35$ . The purpose of this experiment is to show that the algorithm scales gracefully as the number of quadrotors used in the swarm increases. The average risk, average sensor quality, and average number of iterations between 90% cumulative coverage were collected to show how the algorithm scales as the number of quadrotors increases.

Fig. 6 shows the average risk and sensor quality for the swarm as the number of quadrotors increased. For the graph, we averaged the average risk for each of the three scenes for each of the scene sizes. This allows us to get a better picture of the trend as the number of quadrotors increases. Fig. 6 shows the number of quadrotors has little effect on the average associated risk and average sensor quality. We also see that the size of the scene has little effect on these metrics. The figure shows that the average associated risk is under 0.1 (10% risk) for any number of quadrotors and that the average sensor quality is over 0.6 (60% sensor quality) for any number of quadrotors. Therefore, the algorithm is meeting two of the three prescribed task, maintaining high sensor quality whilst maintaining low risk.

We also needed to quantify the persistence of the coverage as the number of quadrotors increased. This is shown in Fig. 7. We can see that average number of iterations it takes for the algorithm to reach 90% cumulative coverage decreases exponentially as the number of quadrotors increases then converges. We also see that the algorithm fills the area more quickly for smaller scene sizes, as expected. The graph shows that the algorithm is able to provide persistent coverage over a given area. To give some context for this graph, if the average cumulative convergence metric was 100 iterations for 5 quadrotors on a 20m by 20m area and it takes 0.5s per iteration and we run the algorithm for 750 iterations, the quadrotors reach 90% cumulative coverage 7.5 times over this  $400 m^2$  area. On average it takes 50s to reach this 90% convergence. Also keep in mind that the speed of the quadrotors was capped at 0.4 meters per iteration, or in this case, 0.8 meters per second. This quick convergence combined with the data from Fig. 6 shows that the algorithm is able to maintain persistent coverage of the area whilst maintaining low risk and high sensor quality.

### 3.3 Performance as a function of control noise

In order to determine if the algorithm would be able to withstand an acceptable amount of error in the controller, we have conducted experiments to test the performance by changing the amount of noise that is present in the simulated proportional-integral-derivative (PID) controller. We did this by adding Gaussian noise to the control output of the PID controller. The noise was quantified

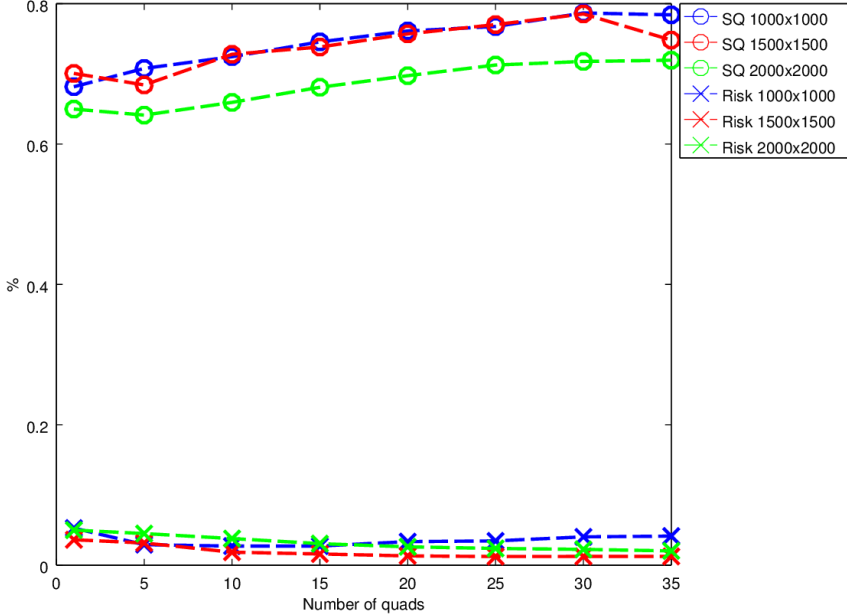


Figure 6: Figure showing how risk and sensor quality relate to the number of quadrotors

by altering the standard deviation of the Gaussian function. For the experiments, the mean for the Gaussian was set to zero and the standard deviation was set from 0 to 0.6 meters with a step of 0.2 meters. This range of values seemed to be an accurate representation of the control noise present on the AscTec Pelicans we used for the practical experimentation. For the experiments, only one scene size was used ( $1500 \times 1500$ ) but three different scenes of that size were used. The number of quads used was 10, 20, and 30 which gave a good overall depiction of the algorithm. The resultant performance information was gathered and averaged. Fig. 8 shows trends for the three different swarm sizes that were used and how the control noise affected the risk and sensor quality.

Fig. 8 shows that the control noise does not affect the performance of the algorithm in terms of the associated sensor quality and risk. Since the algorithm is purely reactive, we can see that within an acceptable amount of noise, that the algorithm is still able to perform well based on the metrics we have used.

Fig. 9 shows that the control noise does not affect the how persistent the coverage is. This is yet another benefit of the algorithm being purely reactive.

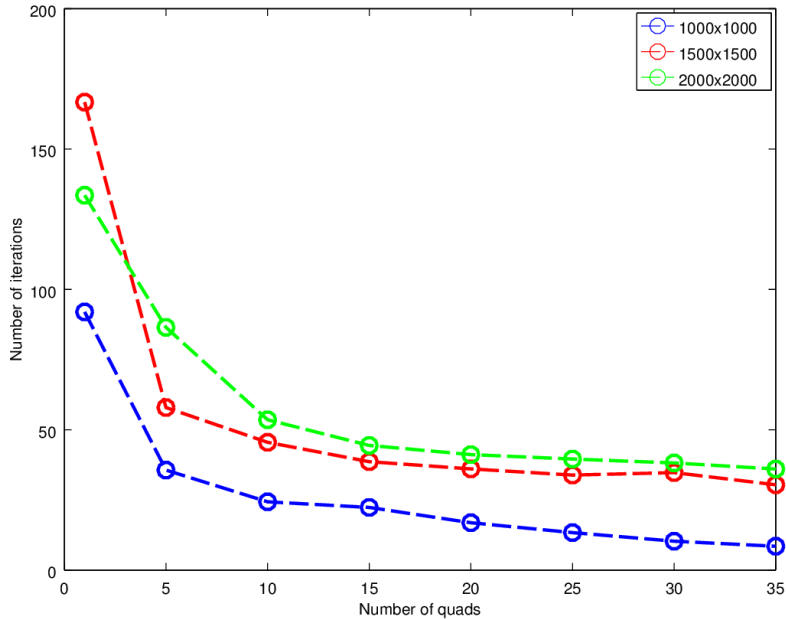


Figure 7: Figure showing the average number of iterations needed to reach 90% cumulative coverage

### 3.4 Computational Efficiency

In order to show that the algorithm can run in a real-time scenario we have graphed the how long each iteration takes to execute as a function as the size of the swarm increases. The figure on the left in Fig. 10 shows this trend. We see a linear increase in the amount of time to plan every the entire swarm for each iteration. The figure on the right in Fig. 10 shows how the time per iteration per quadrotor increases as the number of quads in the swarm increases. We see that if we used a decentralized approach, the amount of time per iteration becomes quite manageable.

### 3.5 Practical Experiments

We tested the algorithm at the Laboratory for Autonomous Systems Research located at the Naval Research Laboratory in Washington DC. We used two AscTec Pelican quadrotors that were operated in a 5.2 meter by 5.2 meter area surrounded by 10 Vicon motion capture cameras. The quadrotors were equipped with with passive motion capture markers which were seen by the Vicon cameras. The Vicon cameras have LEDs which were used to illuminate the passive markers. The 3D positions and the orientations of the quadrotors

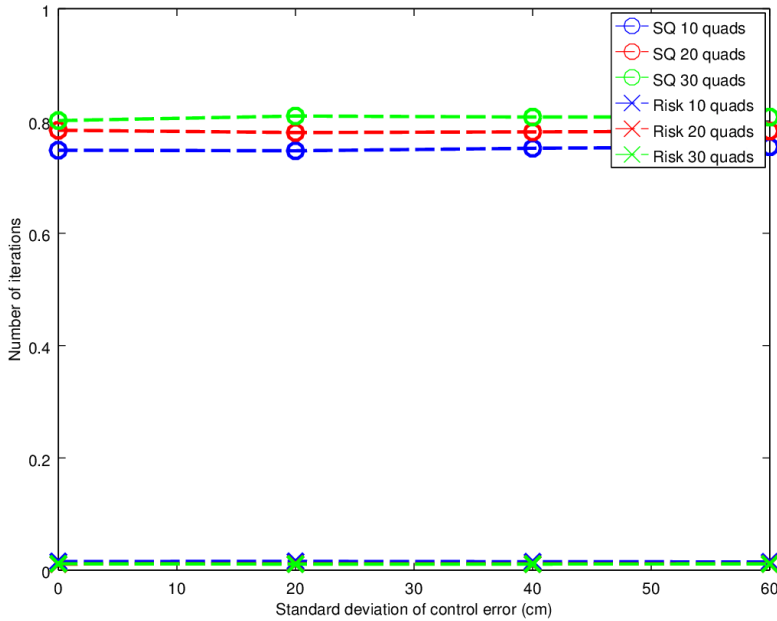


Figure 8: The trend shows how the control noise can affect the risk and sensor quality performance of the algorithm for different swarm sizes

were sent to a laptop which uses the Robotic Operating System (ROS) and a swarm middleware called ZeroMQ-ROS to compute the control commands and to send them to the vehicles. ROS is a open-source middleware combined with software libraries and tools to build robotic applications. ZeroMQ-ROS is a middleware for controlling a swarm using a ROS multi-master architecture. The control commands were sent over WiFi through a socket to each of the quadrotors.

## References

- [1] A. Fournier, D. S. Fussell, and L. C. Carpenter, “Computer rendering of stochastic models,” *Commun. ACM*, vol. 25, no. 6, pp. 371–384, 1982.
- [2] L. Murphy and P. Newman, “Risky planning: Path planning over costmaps with a probabilistically bounded speed-accuracy tradeoff.” in *IEEE International Conference on Robotics and Automation, ICRA 2011, Shanghai, China, 9-13 May 2011*. IEEE, 2011, pp. 3727–3732. [Online]. Available: <http://dx.doi.org/10.1109/ICRA.2011.5980124>

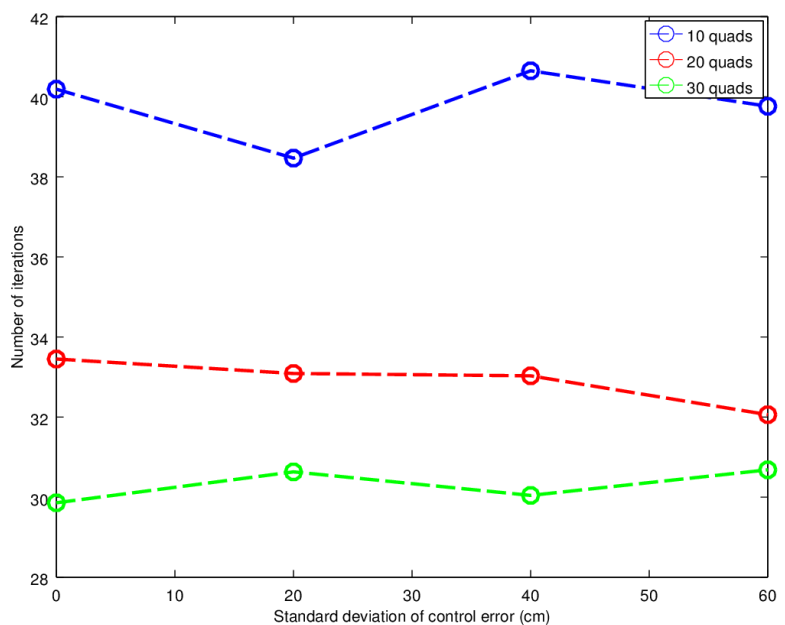


Figure 9: The trend shows how the control noise affects the cumulative coverage rate

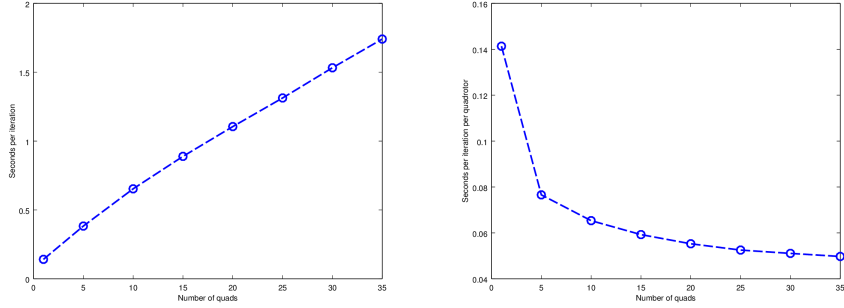


Figure 10: The first figure shows how the amount of time per iteration increases as the number of quadrotors in the swarm increases. The second figure shows how the amount of time per iteration per quadrotor changes as a function of the number of quadrotors.

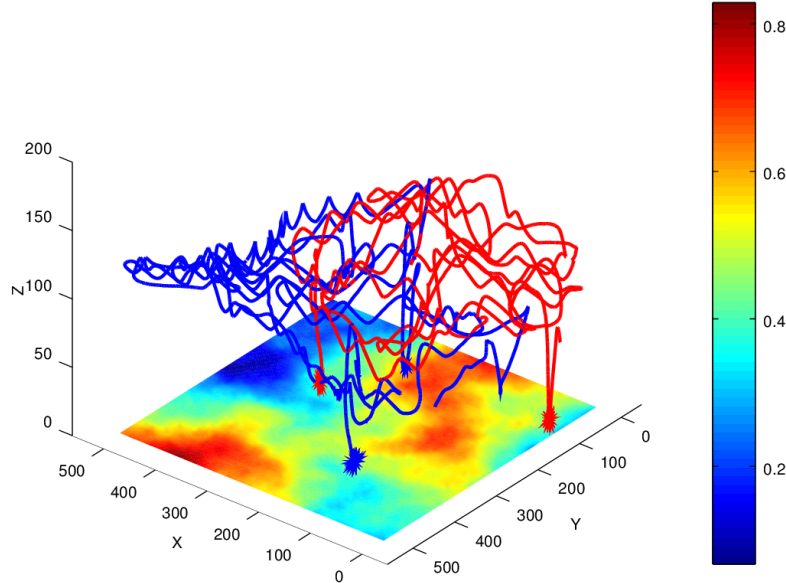


Figure 11: Shows the trajectories for the practical experiments that were run using the AscTec Pelicans at the Laboratory for Autonomous Systems Research at the Naval Research Laboratory. The oscillations shown are caused by the control noise.